Nonlinear Dyn (2017) 90:1987–2000
DOI 10.1007/s11071-017-3775-8

ORIGINAL PAPER

Propagation of surface breathing cracks in shafts under quasi-static rotary bending

P. Rubio · L. Rubio · B. Muñoz-Abella

Received: 17 May 2016 / Accepted: 28 August 2017 / Published online: 6 September 2017

Abstract Due to cyclic loading conditions, cracks frequently appear in rotating machines. The propagation of fatigue cracks in shafts can provoke severe accidents with high risks of people. During the rotation of the cracked shaft, the crack opens and closes in what is called the breathing mechanism, and consequently the behavior of the shaft becomes nonlinear. In the present paper, the propagation of a semi-elliptical crack contained in a rotating shaft has been analyzed considering the nonlinear effect of the crack as the shaft rotates. To this end, an integration algorithm which allows obtaining the crack front evolution has been improved. This procedure uses the Paris-Erdogan Law to determine the advance at a few points along the crack front and uses the general expression proposed previously by the authors that gives the Stress Intensity Factor along the crack front of an elliptical crack in a rotating shaft in terms of the crack depth ratio, the crack aspect ratio, the relative position on the front and the angle of rotation. Several initial semi-elliptical surface crack geometries have been analyzed. For each geometry, the evolution of the crack front has been studied, analyzing the variation of the crack aspect ratio against the crack depth ratio. By the moment, no fatigue growth analyses of surface cracks in rotating shafts, taking into account the breathing mechanism and considering the nonlinear behavior of the shaft, have been found in the literature.

Keywords Cracked shafts · Fatigue crack growth · Elliptical cracks · Breathing mechanism · Rotating shafts

P. Rubio (✉) · L. Rubio · B. Muñoz-Abella
Department of Mechanical Engineering, University Carlos III of Madrid, Avda. Universidad 30, 28911 Leganés, Madrid, Spain
e-mail: prubio@ing.uc3m.es

L. Rubio
e-mail: lrubio@ing.uc3m.es

B. Muñoz-Abella
e-mail: mmunoz@ing.uc3m.es

1 Introduction

Rotating machines as turbines, propellers, rotors and compressors are commonly used in almost all industries and industry processes in general. Shafts, which are one of their main components, work in rotation and are subjected to the action of bending loads. The presence and propagation of fatigue cracks are the major sources of failure for these mechanical elements. Surface cracks can initiate and grow during the service life of the machine, until it cannot stand the stresses and strains and a catastrophic fracture failure occurs. Therefore, the fatigue growth analysis of surface cracks is taking great importance to guarantee the structural safety of these components.

An important aspect to take into account in the dynamic behavior of cracked shafts is the state of the crack during the shaft rotation. There are many works in which the cracks are supposed to be always open [1,2]. The opening and closing of the crack has been

simulated using two well-known models. The first one is the switching crack model, in which the contribution of the crack to the flexibility of the shaft varies from one corresponding to the fully open state to zero corresponding to the fully closed state. It considers that the crack remains either fully open or fully closed, so that the crack is open during half rotation and it is closed during the other half rotation [3–8]. The second one is the breathing crack model, in which the stiffness variation of the shaft is gradual and it takes into account the partial opening and closing of the crack. This model has been studied, numerically or analytically, by different authors [9–21].

The Stress Intensity Factor (SIF) is a parameter that characterizes the stress fields at the crack front. In the case of rotating shafts in which the breathing mechanism takes place the SIF varies for every angle of rotation, passing from positive values when the crack is open to null values when the crack is closed. The crack propagates when the SIF reaches a critical value, denominated fracture toughness which is a material property. Many SIF solutions for surface cracks in non-rotating shafts have been obtained by using several methods: numerical methods [22–31], analytical ones [27,32] and experimental techniques [32–34].

When a shaft rotates, the crack gradually opens and closes, therefore the behavior of the shaft becomes nonlinear [12,14–16,18,19,35–37]. The linear or nonlinear cracked shaft behavior depends on the state of opening and closing of the crack during the shaft rotation. When the crack is fully open, the behavior can be considered linear. However, when the crack is partially open or closed the nonlinear behavior of the cracked shaft takes place. Some researchers have studied the SIF along the crack front in rotating shafts considering the breathing, but not considering the nonlinear behavior [38,39]. Rubio et al. [21] studied the SIF considering that a breathing crack being present in a rotating shaft causes nonlinear behavior. They developed a general expression that gives the SIF along the crack front of an elliptical crack in a rotating shaft considering the behavior of the shaft as a sequence of linear and nonlinear phases each of them characterized by the different states of the crack. Moreover, there are other aspects that can change the regular breathing of the crack in the rotation, causing even the total closing or opening of the crack, for example unbalances and misalignments [20,40].

The crack growth rate depends on the SIF range as is described by the well-known Paris law. Therefore, once the SIF variation along the crack front during one rotation is known, it is possible to analyze the crack propagation. Several studies have been reported to predict the fatigue growth and the remaining fatigue life of surface cracks in round bars. Most of these studies have used the Paris-Erdogan Law to model the growth of the crack, considering that every point at the crack front advances in a perpendicular direction to the front. Carpinteri [41] analyzed the propagation of a surface crack in a round bar under cyclic axial loading with constant amplitude. On the other hand, the same author in a later work [38], studied the propagation of a surface crack in a cylindrical shaft subjected to rotary bending using a two parameter theoretical model. Lin and Smith [42] analyzed the crack front evolution of surface cracks in round bars subjected to axial load and determined the new crack front using a cubic spline approximation. Toribio et al. [43] developed a model of the crack front evolution for a semi-elliptical surface crack in round bars subjected to cyclic axial loading and cyclic bending moment using the SIF expression proposed by Shin and Cai [29]. They generated the new crack front by means of the Least Square Method. Other researchers have used the Forman et al. model [44,45] to analyze the growth of cracks in shafts, although its use is not widespread due to its complexity.

In this paper, the propagation of a semi-elliptical surface crack contained in a shaft under quasi-static rotary bending has been analyzed taking into consideration the nonlinear behavior of the shaft due to the opening and closing of the crack. In the knowledge of the authors, no previous analyses of this type have been found in the literature. Therefore, it highlights the need of analyze the crack propagation considering the nonlinear effects of the breathing crack in rotating shafts. For this, an integration algorithm of the Paris law which allows obtaining the crack front evolution has been improved. Different crack depths and front shapes have been used. It has been assumed that every point at the crack front advances according to a Paris-Erdogan Law. A four-parameter expression which depends on the crack depth ratio, the crack aspect ratio, the position on the front and the angle of rotation that takes into account the breathing mechanism and the nonlinear behavior [21] has been used to determine the SIF. The algorithm has been validated through the comparison with the results reported in other works. In this

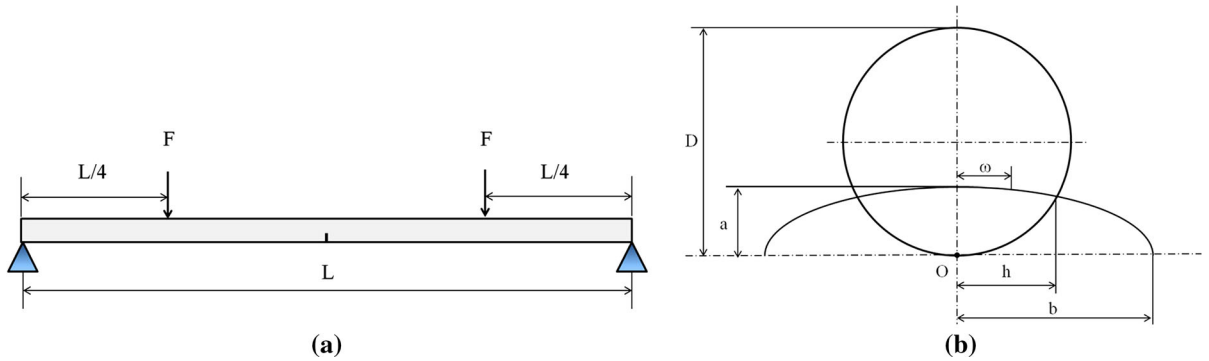

Fig. 1 Geometric model. **a** Crack and loads locations; **b** Parameters of the elliptical front of the crack

work, the evolution of the crack front considering the opening/closing state of the crack has been obtained.

2 Geometric model

The study has been developed using a shaft made of aluminum with the following material properties: Young's Modulus $E = 72$GPa, Poisson's ratio $\nu = 0.3$ and density $\rho = 2800\,\text{kg/m}^3$. The shaft total length is $L = 900$ mm, whereas the diameter is $D = 20$ mm. The transversal elliptical crack, of depth a, is located at the center of the shaft. The shaft is submitted to two loads, $F = 100$ N, which have been located at a distance $\frac{L}{4}$ far away from both ends of the shaft as can be seen in Fig. 1a. The crack front has been modeled as an ellipse with center O located at the shaft surface; semi minor axis a and semi major axis b (see Fig. 1b). The geometric parameters which define the elliptical shape of the crack are: the nondimensional crack depth (depth ratio) $\alpha = \frac{a}{D}$; the nondimensional crack shape (shape ratio) $\beta = \frac{a}{b}$; and the relative position on the crack front $\gamma = \frac{w}{h}$ (Fig. 1b). The elliptical crack front has been discretized in twelve equal segments according the relative positions on the front γ which varies from -1 to 1.

3 Dimensionless SIF

The dimensionless SIF employed in the algorithm has been obtained from the general expression proposed by the authors in a previous paper [21] which considers the breathing mechanism and the nonlinear behavior when the crack opens and closes.

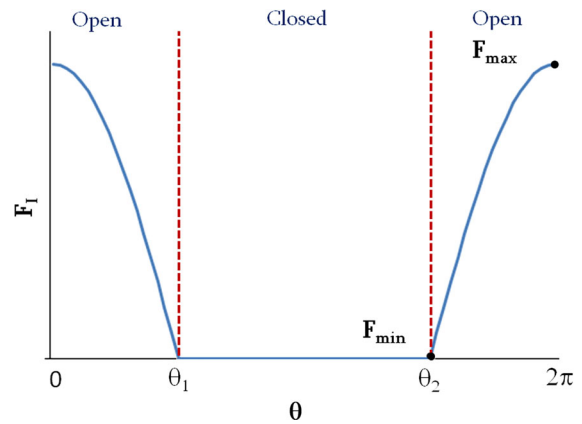

Fig. 2 Evolution of the SIF for a generic point γ during a rotation

Rubio et al. [21] carried out a 3D quasi-static numerical study, through the Commercial Code ABAQUS [46] to obtain the SIF along the crack front of a shaft subjected to rotary bending. From the numerical results, a polynomial expression of the SIF, which is a function of the crack depth ratio α, the crack shape ratio β, the relative position on the crack front γ and the rotation angle θ was obtained. During the breathing, the crack passes from the closed state to the open state gradually in a rotation causing the nonlinear behavior of the shaft [16,17,19,47]. The expression was determined taking into account this situation. Figure 2 shows the nondimensional SIF, F_I, versus rotation angle θ for a generic location on the front γ and for a generic crack depth α and shape β. It can be seen the evolution of SIF, including the maximum and minimum SIF during a rotation. For a given location on the front γ, the crack remains open until $\theta = \theta_1$ (the SIF is positive), angle in which that point on the front closes. Between θ_1 and

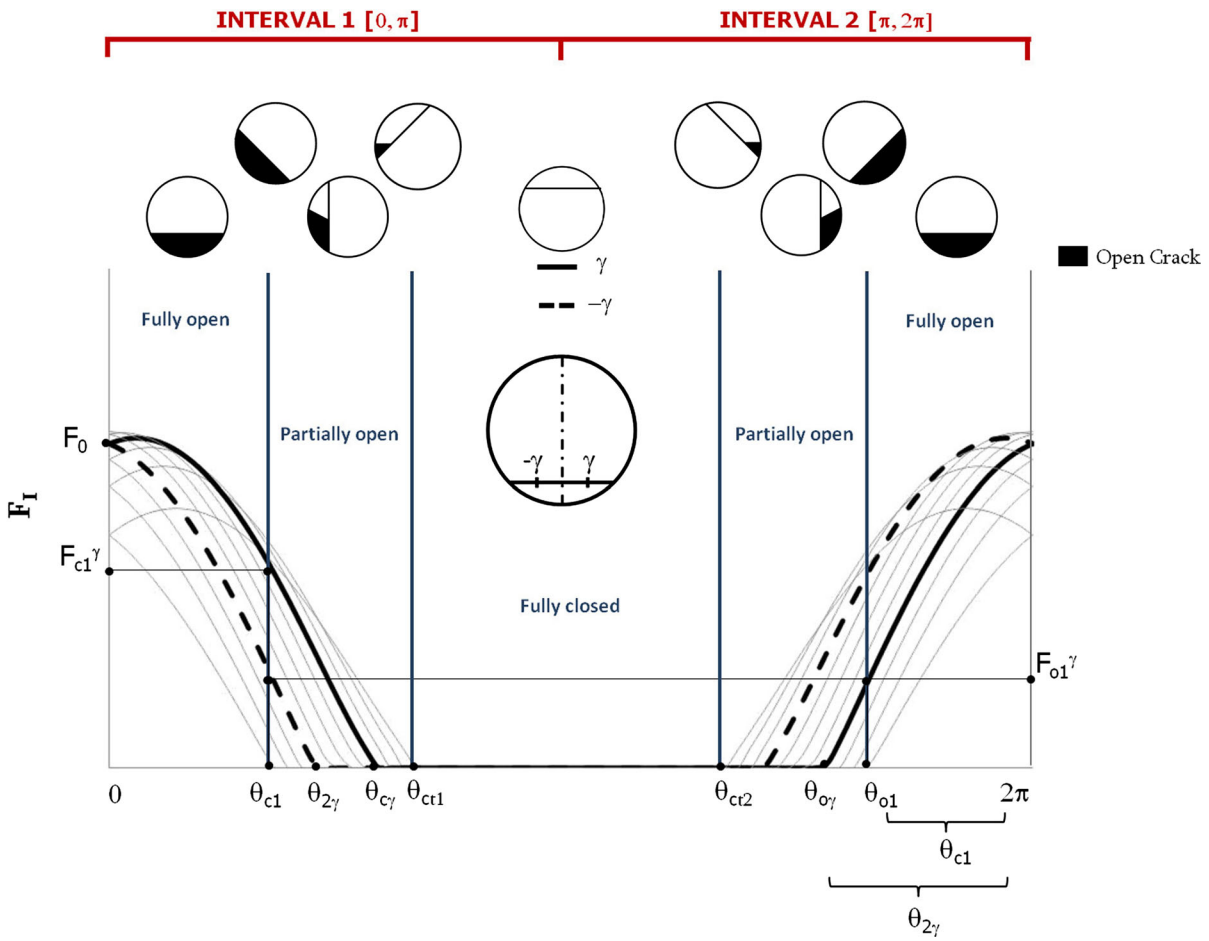

Fig. 3 Nondimensional SIF versus rotation angle θ for each position on the crack front in a generic geometry crack [21]

θ_2 the crack is closed (the SIF is null). Finally, when the shaft reaches the angle θ_2, the crack opens again (the SIF is positive again).

Similarly, in Fig. 3, it can be seen the evolution of the nondimensional SIF, F_I, versus rotation angle θ considering the different locations on the front γ (different curves) for a generic crack depth α and shape β. Two rotation intervals were considered: from 0 to π (Interval 1) and from π to 2π (Interval 2). The black continuous line represents the SIF evolution corresponding to the generic position on the front γ and the black dotted line represents the SIF evolution for the generic position on the front $-\gamma$. The shaft rotates in a clockwise direction.

To determine the SIF expression, some variables were defined according to Fig. 3:

- θ_{c1} is the rotation angle in which the crack front starts to close.
- $\theta_{c\gamma}$ is the first rotation angle, for a given location on the front γ, in which F_I is null (when that point on the crack front closes).
- $\theta_{2\gamma}$ is the first rotation angle, for a given location on the front $-\gamma$, in which F_I is null (when that point on the crack front closes).
- $\theta_{o\gamma}$ is the last rotation angle, for a given location on the front γ, in which F_I is null (when that point on the crack front opens).
- θ_{o1} is the rotation angle in which the crack front is fully open again, because all the F_I values on the crack front are positive.
- θ_{ct1} is first rotation angle in which the crack front is fully closed.
- θ_{ct2} is last rotation angle in which the crack front is fully closed.

Regarding the values of the SIF:

- F_0 is the F_I value for the rotation angle $\theta = 0$ for a given location on the front γ.
- F_{c1}^{γ} is the F_I value for the rotation angle $\theta = \theta_{c1}$ for a given location on the front γ.
- F_{o1}^{γ} is the F_I value for the rotation angle $\theta = \theta_{o1}$ for a given location on the front γ.

To determine these variables, some polynomial expressions were obtained by using multiple regression techniques and taking into account all the numerical results. These expressions can be found in [21].

From these variables, three SIF expressions were determined for each interval. Firstly, when the crack is fully open, the nondimensional SIF, called $F_{I,1}^{\mathrm{FO}}$ and $F_{I,2}^{\mathrm{FO}}$, were calculated through a simple linear combination of sines and cosines as follows:

$$F_{I,1}^{\mathrm{FO}}(\alpha,\beta,\gamma,\theta) = A_1\cos\theta + B_1\ \sin\theta \quad \text{(Interval 1)} \tag{1}$$

$$F_{I,2}^{\mathrm{FO}}(\alpha,\beta,\gamma,\theta) = A_2\cos\theta + B_2\ \sin\theta \quad \text{(Interval 2)} \tag{2}$$

where FO means Fully Open, 1 and 2 represent the intervals, and A_1, B_1, A_2 and B_2 are constants which depend on the variables mentioned before and that can be found in [21].

Secondly, when the crack is partially open, the behavior of the shaft is nonlinear and the nondimensional expressions of the SIF were obtained:

$$F_{I,1}^{\mathrm{PO}}(\alpha,\beta,\gamma,\theta) = C_1\theta^3 + D_1\theta^2 + E_1\theta + H_1 \quad \text{(Interval 1)} \tag{3}$$

$$F_{I,2}^{\mathrm{PO}}(\alpha,\beta,\gamma,\theta) = C_2\theta^3 + D_2\theta^2 + E_2\theta + H_2 \quad \text{(Interval 2)} \tag{4}$$

where PO means Partially Open, C_1, D_1, E_1, H_1, C_2, D_2, E_2 and H_2 are constants that also depends on the previous variables [21].

Finally, when the crack is fully closed, the values of the SIF are always null:

$$F_{I,1}^{\mathrm{FC}}(\alpha,\beta,\gamma,\theta) = 0 \tag{5}$$

$$F_{I,2}^{\mathrm{FC}}(\alpha,\beta,\gamma,\theta) = 0 \tag{6}$$

where FC means Fully Closed.

4 Crack front evolution

In order to analyze the propagation of a crack contained in a rotating shaft, a propagation algorithm have been developed to determine iteratively the geometric evolution of the crack front.

The proposed model has been based on the assumption that the crack front can be modeled as an ellipse. Likewise, the model assumes that the crack front advances according to the Paris-Erdogan Law as in many other works [25,26,41–43,48–50]:

$$\frac{\mathrm{d}a}{\mathrm{d}N} = C\Delta K_I{}^m \tag{7}$$

where $\frac{\mathrm{d}a}{\mathrm{d}N}$ is the crack propagation rate which is expressed in m/cycle; ΔK_I is the Stress Intensity Factor range which is expressed in $MPa\sqrt{m}$; C y m are constants of the Paris Law which depend on the material. In this case, the material of the shaft is aluminum and the material constants are: $C = 45\text{x}10^{-9}$ and $m = 2.9$.

To discretize the elliptical crack front, it has been divided into twelve equal segments according to the relative positions on the front γ which varies from -1 to 1.

The SIF at each point of the crack front have been determined according to equation:

$$K_I = F_I\sigma\sqrt{\pi a} \tag{8}$$

where σ is the reference stress which has been taken as the maximum bending stress of the uncracked shaft, and F_I is the nondimensional SIF previously mentioned in Sect. 3.

Once the SIF has been obtained at each point of the crack front for the whole rotation, the SIF range at this point has been determined as follows [38]:

$$\Delta K_{\mathrm{I,\,whole\,rotation}} = K_{I,\,\max} - K_{I,\,\min} \tag{9}$$

where $K_{I,\,\max}$ and $K_{I,\,\min}$ are, respectively, the maximum and minimum values of the SIF during the rotation.

Therefore, according to Fig. 2, the SIF range at the considered point is equal to the maximum value of the SIF in the rotation.

The crack advance, Δa, is obtained by integrating the Paris-Erdogan Law, and for any point can be expressed in the following form:

$$\Delta a = \Delta N \cdot C \cdot [\Delta K_I]^m \tag{10}$$

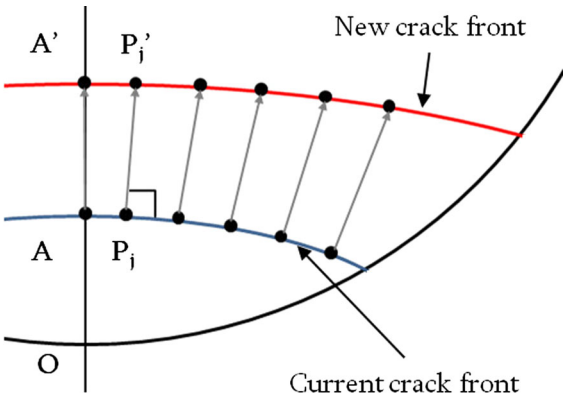

Fig. 4 Local crack advances along the crack front

where ΔN is the number of cycles required to reach a certain value of Δa.

For two points of the front, the point located at the crack center (A) and another point (P_j), the crack depth variation is given by the following expressions (Fig. 4):

$$\Delta a(A) = \Delta N \cdot C \cdot [\Delta K_I(A)]^m \tag{11}$$

$$\Delta a(P_j) = \Delta N \cdot C \cdot [\Delta K_I(P_j)]^m \tag{12}$$

where j is the number of points along the crack front.

The crack advance at each point of the crack front $\Delta a(P_j)$ can be written:

$$\Delta a(P_j) = \Delta a(A) \left(\frac{\Delta K_I(P_j)}{\Delta K_I(A)} \right)^m \tag{13}$$

where $\Delta a(A)$ is the advance at the crack center which has been given an initial value as it is indicated further in the text.

From the obtained points, A' and P'_j, a new elliptical front with semi-axes a' and b', has been fitted by the

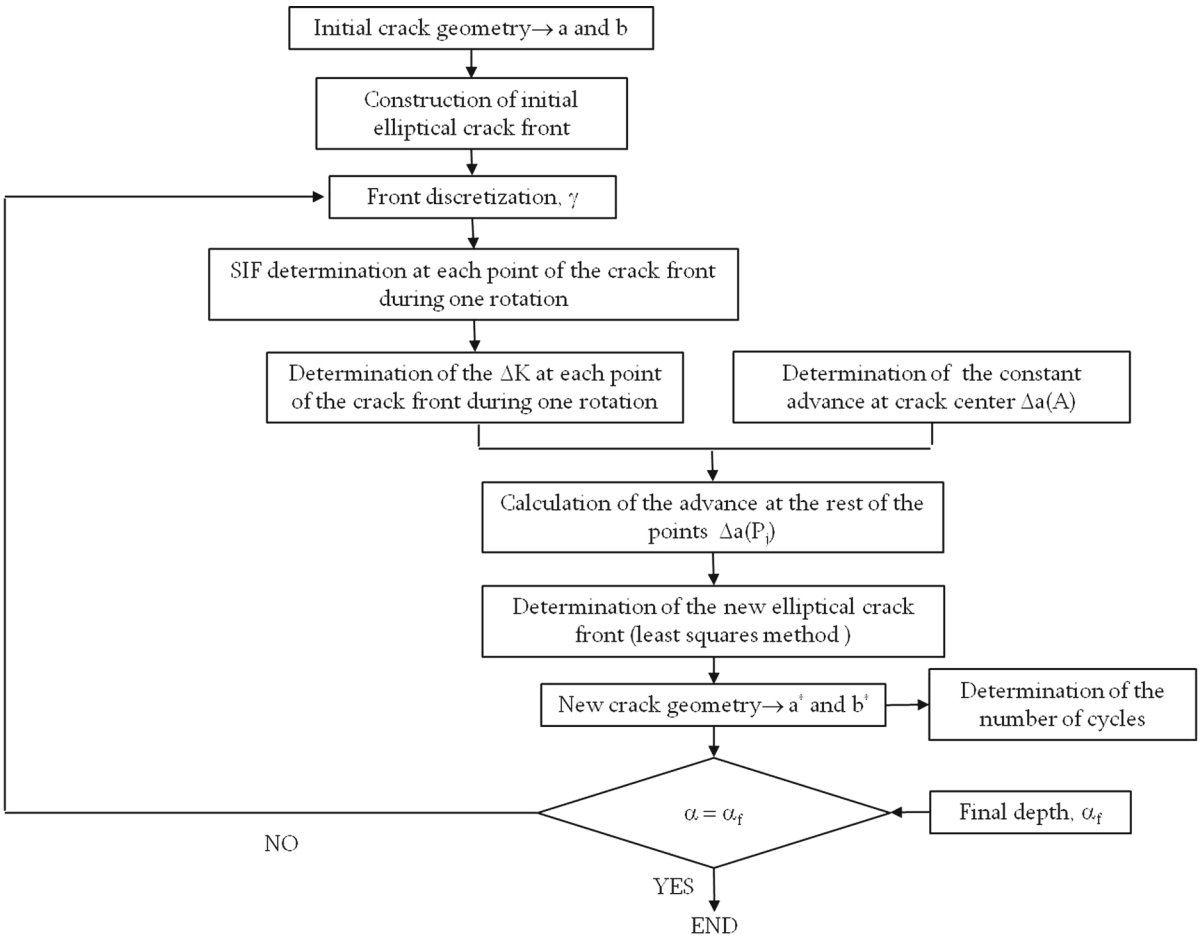

Fig. 5 Flowchart of the procedure

Least Squares Method. The process has been repeated iteratively until the crack depth reaches a fixed value.

The developed algorithm allows calculating the number of cycles for a prefixed advance $\Delta a(A)$ at each iteration, or calculating the advance $\Delta a(A)$ for a prefixed number of cycles at each iteration. In this paper, the advance at crack center has been imposed, according to the sensitivity analysis explained later, remaining constant from one iteration to another. On the other hand, the number of cycles has been determined for each iteration, considering the front shape variation of the previous iteration:

$$N_i = \int_{a_i}^{a_i+\Delta a(A)} \frac{da}{C\Delta(K^i_{I\,\max}(A))^m} \tag{14}$$

where a_i is the initial crack depth and $\Delta K^i_{I\,\max}(A)$ is the SIF variation of the point A at each iteration.

Hence, the total number of cycles required to reach a final depth of the crack α_f can be obtained by adding the cycles calculated at each iteration:

$$N_T = \sum_{i=1}^{\text{iter}} N_i \tag{15}$$

where i is the number of iterations and iter is the total number of iterations.

In Fig. 5 a flowchart of the procedure is shown.

In order to determine the optimal value of the advance at crack center $\Delta a(A)$ which remains constant during the integration, a sensitivity analysis of the $\Delta a(A)$ has been made. In Fig. 6, the results of study of the convergence are given. The crack aspect ratio β, versus crack depth ratio α have been plotted for the different values of the advance. Each figure shows the evolution of the crack for a given initial aspect β_0 and depth ratio α_0. As can be observed, for every $\Delta a(A)$ if the initial crack aspect ratio is $\beta_0 = 0$, the aspect ratio increases until a certain depth value, and then decreases to zero. Therefore, the crack becomes more elliptical at first and then, it becomes straighter. If $\beta_0 = 1$, the aspect ratio decreases until reaching zero value, it is to say, the crack becomes straight with the growth. According to this analysis, there is a good agreement between the curves corresponding to $\Delta a(A) = 0.5\%$ and 0.33% of the diameter. So, the value of the fixed advance equal to 0.5% of the diameter is adequate to be used in the computations.

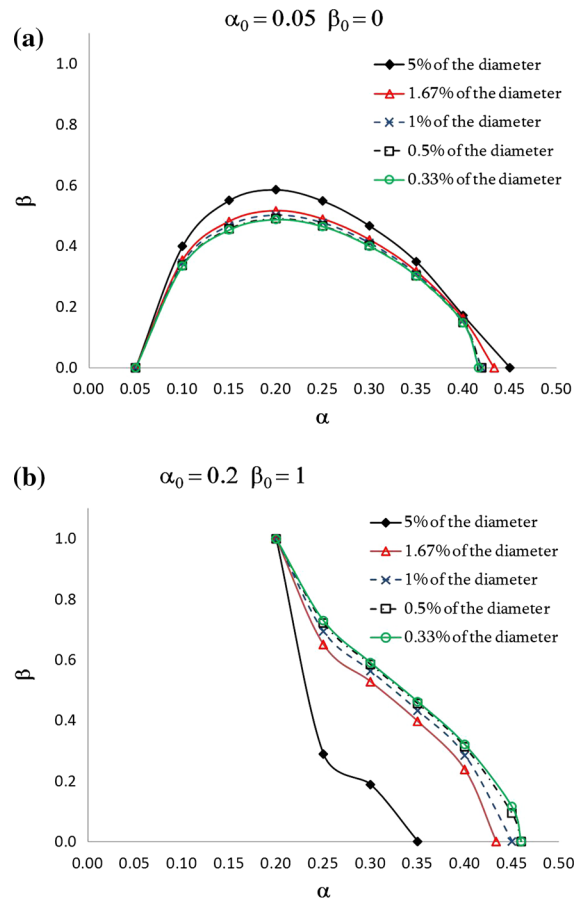

Fig. 6 Sensitivity analysis for different $\Delta a(A)$. **a** $\alpha_0 = 0.05$ $\beta_0 = 0$; **b** $\alpha_0 = 0.05$ $\beta_0 = 1$

5 Validation of the propagation model

In order to validate the propagation algorithm developed, some results of the geometrical evolution of the crack front have been compared with some data available in the literature [38,43]. Firstly, when the shaft is subjected to pure bending and the crack is totally open, the model has been validated through the comparison with the results reported by Toribio [43]. Secondly, when the shaft is subjected to rotary bending the results of the proposed model have been compared with that obtained by Carpinteri [38].

Toribio et al. [43] developed a numerical model of the crack front evolution for elliptical surface crack in round bars subjected to bending, that can be used only when the crack is totally open. The dimensionless SIF employed in their computations is that proposed by Shin and Cai [29]. In this case, rotation angles were not

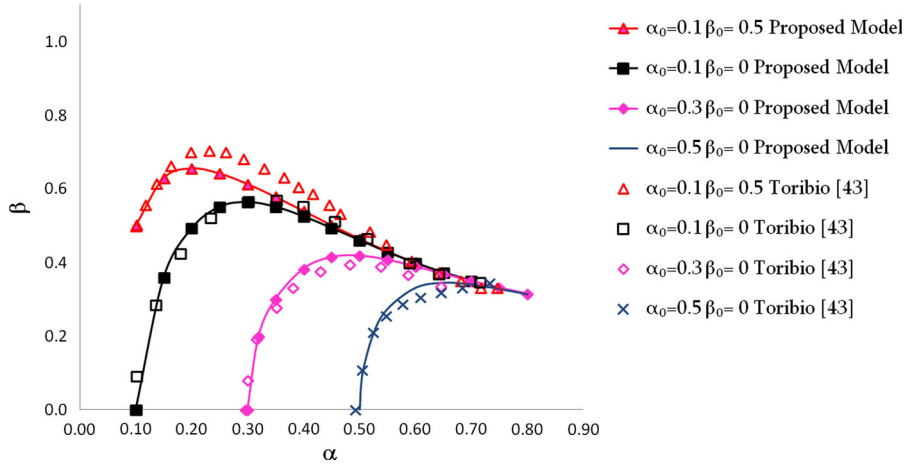

Fig. 7 Comparison between the predictions of the present model and results obtained by Toribio et al. [43] when the crack is completely open (bending loading)

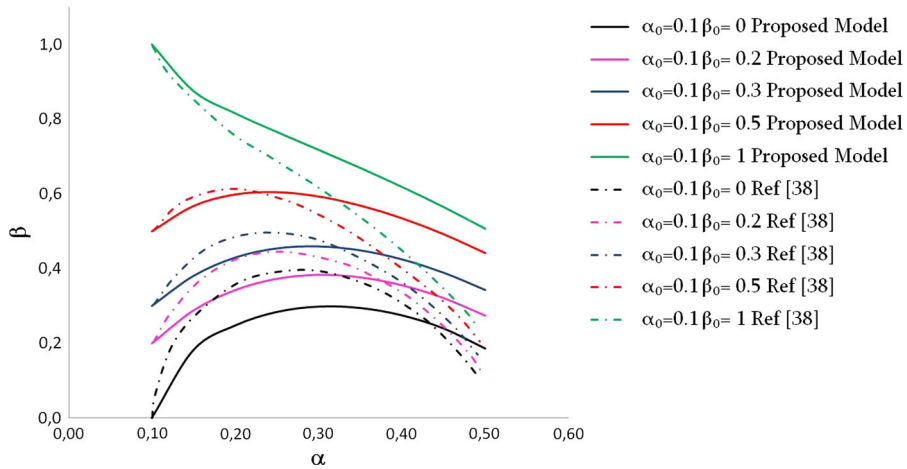

Fig. 8 Comparison between the predictions of the present model and the results obtained by Carpinteri [38] under rotating bending

being taken into account. In Fig. 7, the results from the proposed model when the crack is totally open have been compared with those obtained by Toribio et al. [43] for an exponent of the Paris Law $m = 3$ and for different initial geometries. The initial geometries that have been used in the comparison are: $\alpha_0 = 0.1$ and $\beta_0 = 0$; $\alpha_0 = 0.3$ and $\beta_0 = 0$; $\alpha_0 = 0.5$ and $\beta_0 = 0$; $\alpha_0 = 0.1$ and $\beta_0 = 0.5$. It is clear that the results are in good agreement. In both models, for the initial studied geometries the crack becomes more elliptical until certain depth and then becomes straighter until the shape crack ratio reaches the value $\beta = 0.3$. The curves corresponding to the initial geometry $\alpha_0 = 0.1$ $\beta_0 = 0$, $\alpha_0 = 0.3$ $\beta_0 = 0$ and $\alpha_0 = 0.5$ $\beta_0 = 0$ almost coincide. For $\alpha_0 = 0.1$ $\beta_0 = 0.5$, although the curves do not coincide, they always follow the same trend.

Hence, it can be concluded that when the crack is totally open in static conditions, the proposed model for propagation provides good results and, it is considered to be validated.

Secondly, when the shaft is subjected to rotary bending, the opening of the crack changes continuously with the shaft rotation. In this case, the results of the propagation model have been compared with the ones obtained by Carpinteri [38] for an exponent of the Paris Law $m = 2$ (see Fig. 8). The model of Carpinteri [38] is linear. The initial geometries that have been used in the comparison are: $\alpha_0 = 0.1$ and $\beta_0 = 0$; $\alpha_0 = 0.1$ and $\beta_0 = 0.2$; $\alpha_0 = 0.1$ and $\beta_0 = 0.3$; $\alpha_0 = 0.1$ and $\beta_0 = 0.4$; $\alpha_0 = 0.1$ and $\beta_0 = 0.5$. It can be observed that the curves corresponding to both models always follow the same trend. At first, the crack front becomes more elliptical and later becomes straighter with the growth. With the Carpinteri propagation model [38], the shape crack ratio reaches a value which varies from $\beta = 0.12$ to 0.25 for the depth $\alpha = 0.5$ while with the proposed model,

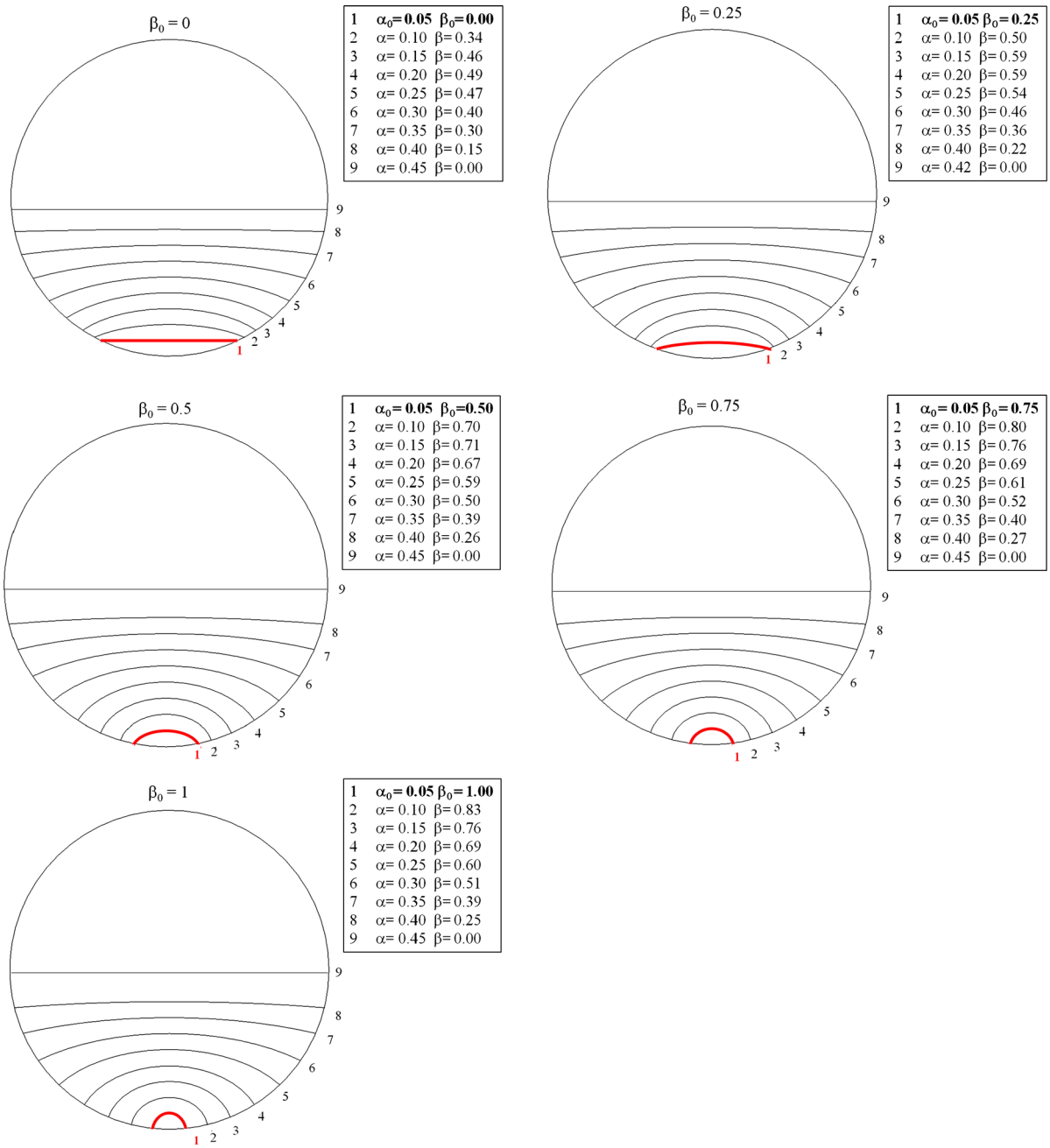

Fig. 9 Crack front evolution for an initial crack depth $\alpha_o = 0.05$ and different values of the initial crack shape ratio

for same depth, the shape crack ratio reaches a value which varies from $\beta = 0.19$ to 0.51. These discrepancies between the two models come from the different expressions used to obtain the dimensionless SIF [21]. In Rubio et al. [21] it was observed that when the crack is completely open the SIF results are similar for both models. However, when the crack is partially open, there are discrepancies in the opening percentages between the two models, for example, for $\alpha = 0.25$, $\beta = 0$ and $\theta = \frac{\pi}{2}$, Carpinteri [38] obtained that exactly half of the crack is open, however, the SIF model of Rubio et al. [21] and other models from the literature

[19] obtained that more than half of the crack is open. Finally, when the crack is closed, the SIF solutions by Carpinteri [38] are the same absolute values as when the crack is open but opposite, while the model [21] considers that these values should be null. This may be because in the SIF determination model [38] the crack faces are interpenetrating giving negative values of the SIF, so they are not considering the nonlinearity of the problem.

Therefore, taking into account the discrepancies between the two SIF determination models mentioned before and the same trend in the results shown, it can be concluded that the propagation model proposed can be also validated for the case of shafts under quasi-static rotary bending.

6 Application of the propagation model: results

In this section, the results that have been obtained by using the developed propagation algorithm of Sect. 5 are shown.

6.1 Evolution of the crack front

Firstly, the evolution of the crack front has been analyzed. In Fig. 9 the crack shape evolution for an initial crack depth ratio $\alpha_o = 0.05$ and different initial crack aspect ratios ($\beta_o = 0; 0.25; 0.5; 0.75; 1$) is shown. It can be observed that regardless of the initial crack aspect ratio, the crack front gradually becomes straight.

The growth for the initial cracks shown in Fig. 9 is also analyzed in Fig. 10. Here the geometrical evolution of the crack front has been shown by plotting the crack aspect ratio β versus the crack depth ratio α. It can be observed that the curves tend to converge, that is, cracks tend to adopt the same front. If the initial crack is straight ($\beta_o = 0$), the crack front gradually becomes more elliptical until certain depth value and then becomes straighter. Otherwise, if the initial crack is circular ($\beta_o = 1$), the crack aspect ratio decreases, that is, the crack tends to become straight with the growth. Similarly, it can be seen that, regardless of the initial geometry, the crack front becomes straight because in any case the crack aspect ratio tends to zero. Figure 11 shows similar results for an initial crack depth ratio greater than $\alpha_o = 0.05$. If the initial depth α_o is less than 0.3 and the initial crack is straight

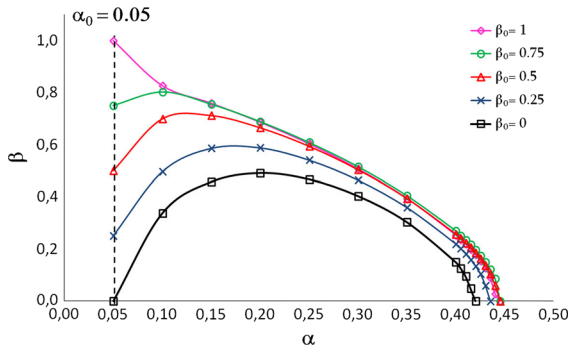

Fig. 10 Crack shape ratio β, against the crack depth ratio α, for an initial crack depth $\alpha_o = 0.05$ and different values of the initial crack shape ratio β_o

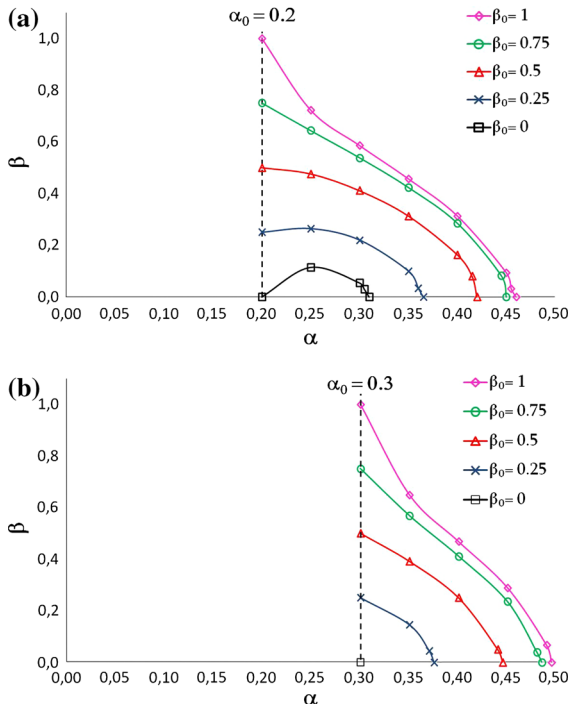

Fig. 11 Crack shape ratio β, versus the crack depth ratio α, for different values of the initial crack shape ratio β_o and the initial crack depth ratio α_o. **a** $\alpha_0 = 0.2$; **b** $\alpha_0 = 0.3$

($\beta_o = 0$), the crack first becomes more elliptical, and later, straighter. When the initial depth α_o is equal to 0.3 and the initial crack is straight ($\beta_o = 0$), the crack front becomes straighter with the growth. Regardless of the depth ratio, if the initial crack is circular ($\beta_o = 1$) the crack becomes straight with the growth.

Although most of the studies on cracked shafts consider convex shaped cracks [26,29,51–56] (Fig. 12a),

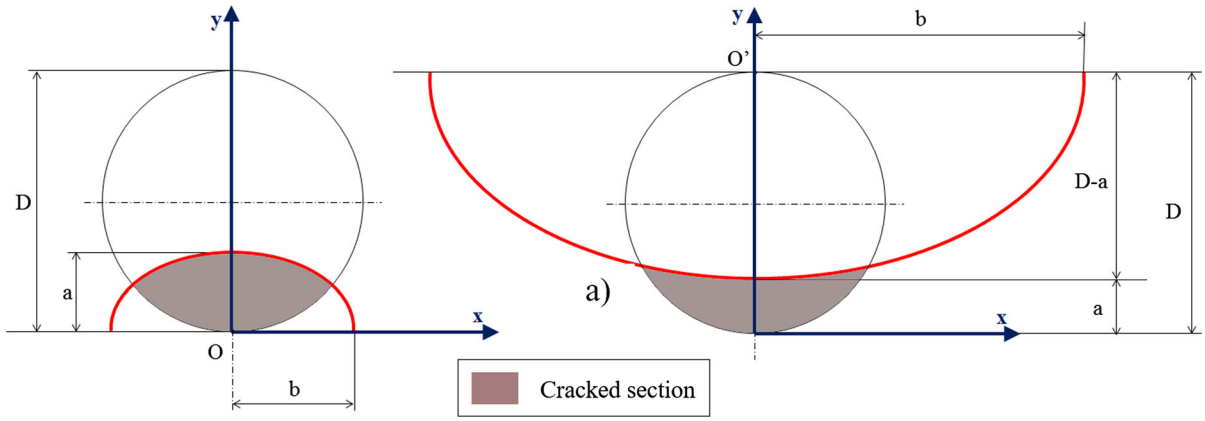

Fig. 12 Typical crack shapes. **a** Convex; **b** Concave

there are a limited number of papers related to concave shaped cracks [57–60] (Fig. 12b). Provided that the SIF in the crack center is greater than in the ends, the crack front will become more elliptical with growth (Fig. 13a). However, when the SIF in the crack center is smaller than in the ends (Fig. 13b), the crack aspect ratio will decrease with the growth and the crack front will become gradually straight until $\beta = 0$. From that moment, it is expected that the crack front shape will change from straight to concave.

In addition, the crack depth ratio in which the crack front shape will probably change from convex to concave for the initial geometries studied, is given in Table 1. For example, for an initial convex crack of $\alpha_0 = 0.2$ and $\beta_0 = 0.25$, the crack will change to concave when $\alpha = 0.36$. As can be seen, the crack front shape changes from convex to concave shape prior if the crack front is initially straighter. In Table 1, "No convex elliptical shape" means that for those straight initial geometries the SIF at the crack center is smaller than the SIF at the ends, so the crack front shape should change directly from straight to concave.

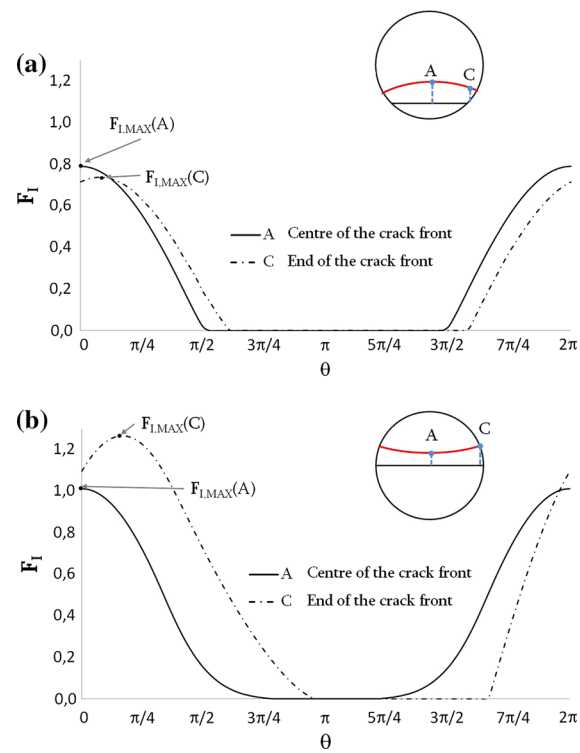

Fig. 13 Maximum SIF at the at the crack center and at the ends. **a** $\alpha = 0$; **b** $\alpha = 0.5$

6.2 Number of cycles

The proposed propagation model also allows to study the number of cycles required to reach a certain depth. In Fig. 14, the number of cycles required for a crack, of initial depth ratio $\alpha_0 = 0.05$, to reach different depths is shown. The number of cycles has been plotted versus the crack depth ratio α for different initial crack aspect ratios ($\beta_0 = 0$; 0.25; 0.5; 0.75; 1). As can be seen, the

Table 1 Crack depth ratio in which the crack front shape changes from convex to concave for the initial geometries

	$\beta_0 = 0$	$\beta_0 = 0.25$	$\beta_0 = 0.5$	$\beta_0 = 0.75$	$\beta_0 = 1$
$\alpha_0 = 0.05$	0.42	0.44	0.45	0.45	0.45
$\alpha_0 = 0.1$	0.38	0.41	0.435	0.445	0.445
$\alpha_0 = 0.15$	0.345	0.38	0.425	0.445	0.45
$\alpha_0 = 0.2$	0.31	0.36	0.42	0.45	0.46
$\alpha_0 = 0.25$	0.27	0.36	0.43	0.465	0.475
$\alpha_0 = 0.3$	No convex elliptical shape	0.375	0.445	0.485	0.495
$\alpha_0 = 0.35$	No convex elliptical shape	0.405	0.47	>0.5	>0.5
$\alpha_0 = 0.4$	No convex elliptical shape	0.45	>0.5	>0.5	>0.5
$\alpha_0 = 0.45$	No convex elliptical shape	0.485	>0.5	>0.5	>0.5

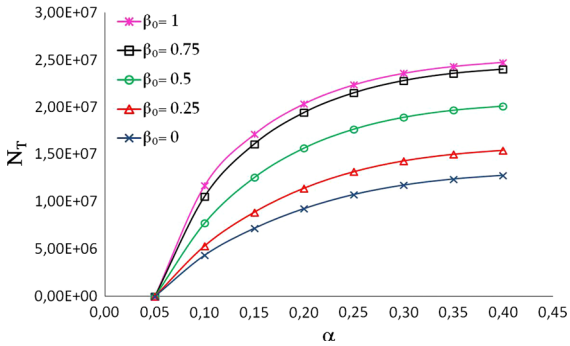

Fig. 14 Number of cycles required for the propagation of an initial crack $\alpha_0 = 0.05$ and different β_0

number of cycles increases when the initial crack shape ratio β_0 is greater. If the initial geometry is circular ($\beta_0 = 1$), the number of cycles is about twice than that obtained for straight geometries. Therefore, the growth of the straight fronted cracks is faster than for the semi-elliptical shaped cracks. Moreover, the slopes of the curves are smaller as the crack is deeper, that is, the growth is slower as the crack is deeper.

The same results are produced for any other initial crack depths α_0.

7 Conclusions

In this work the fatigue crack propagation in quasi-static rotating shafts have been analyzed taking into account the nonlinear effect of the breathing crack. To this end, an integration algorithm which allows obtaining the crack front evolution has been improved. This algorithm assumes that the crack advance at each point of the front follows the Paris-Erdogan Law. The algorithm uses an expression of the Stress Intensity Factor (SIF) (previously obtained by the authors [21]) which takes into account the breathing mechanism and considers the nonlinear behavior of the shaft. To validate the propagation model, a comparison between some results of the present study and results available in the literature has been carried out. It has been found that they are in good agreement. Once validated, the model has been used to analyze the evolution of a semi-elliptical surface crack contained in a rotating shaft. From the obtained results, the following conclusions may be drawn.

Regardless of the initial geometry, the crack front becomes straight with the growth. If the initial crack is straight ($\beta_o = 0$), the crack front gradually becomes more elliptical until certain depth value and then becomes straighter. Otherwise, if the initial crack is circular ($\beta_o = 1$), the crack becomes straight with the growth. Once the crack has adopted a straight shape, the crack front shape will probably change from convex to concave as the advances at crack center are lower than the advances at the ends.

Finally, the number of cycles required for the propagation of the crack increases when the initial crack shape ratio β_0 is greater. Therefore, the growth of the straight fronted cracks is faster than for semi-elliptical shaped cracks.

For the first time, in the present paper, the propagation of a crack contained in a quasi-static rotating shaft has been analyzed considering the opening/closing state of the crack and the nonlinear behavior. To this end, the developments of the work will help to predict, on one hand, the fatigue growth of a crack in

a rotating shaft, and on the other hand, the remaining fatigue life of a cracked shaft.

Acknowledgements The authors would like to thank the Spanish *Ministerio de Economía y Competitividad* for the support for this work through the project DPI2013-45406-P.

References

1. Papadopoulos, C.A., Dimarogonas, A.D.: Coupled longitudinal and bending vibrations of a rotating shaft with an open crack. J. Sound Vib. **117**, 81–93 (1987)
2. Papadopoulos, C.A., Dimarogonas, A.D.: Coupled longitudinal and bending vibrations of a cracked shaft. J. Vib. Acoust. Stress Reliab. Des. **110**, 1–8 (1988)
3. Gasch, R.: A survey of the dynamic behavior of a simple rotating shaft with a transverse crack. J. Sound Vib. **160**, 313–332 (1993)
4. Gasch, R.: Dynamic behavior of the Laval rotor with a transverse crack. Mech. Syst. Signal Process. **22**, 790–804 (2008)
5. Muller, P.C., Bajowski, J., Soffker, D.: Chaotic motions and fault detection in a cracked rotor. Nonlinear Dyn. **5**, 233–254 (1994)
6. Pu, Y.P., Chen, J., Zou, J., Zhong, P.: Quasi-periodic vibration of cracked rotor on flexible bearings. J. Sound Vib. **251**, 875–890 (2002)
7. Qin, W.Y., Meng, G., Zhang, T.: The swing vibration, transverse oscillation of cracked rotor and the intermittence chaos. J. Sound Vib. **259**, 571–583 (2003)
8. Qin, W.Y., Cheng, G., Ren, X.: Grazing bifurcation in the response of cracked Jeffcott rotor. Nonlinear Dyn. **35**, 147–157 (2004)
9. Mayes, I.W., Davies, W.G.R.: Analysis of the response of a multi-rotor-bearing system containing a transverse crack in a rotor. J. Vib. Acoust. Stress Reliab. Des. **106**, 139–145 (1984)
10. Tsai, T.C., Wang, Y.Z.: Vibration analysis and diagnosis of a cracked shaft. J. Sound Vib. **192**, 607–620 (1996)
11. Keiner, H., Gadala, M.S.: Comparison of different modelling techniques to simulate the vibration of a cracked rotor. J. Sound Vib. **254**(5), 1012–1024 (2002)
12. Sinou, J.J., Lees, A.W.: The influence of cracks in rotating shafts. J. Sound Vib. **285**, 1015–1037 (2005)
13. Al-Shudeifat, M.A., Butcher, E.A.: New breathing functions for the transverse breathing crack of the cracked rotor system: approach for critical and subcritical harmonic analysis. J. Sound Vib. **330**, 526–544 (2011)
14. Jun, O.S., Eun, H.J., Earmme, Y.Y., Lee, C.W.: Modelling and vibration analysis of a simple rotor with breathing crack. J.Sound Vib. **155**, 273–290 (1992)
15. Darpe, A.K., Gupta, K., Chawla, A.: Transient response and breathing behavior of a cracked Jeffcott rotor. J. Sound Vib. **272**, 207–243 (2004)
16. Darpe, A.K., Gupta, K., Chawla, A.: Coupled bending, longitudinal and torsional vibrations of a cracked rotor. J. Sound Vib. **269**, 33–60 (2004)
17. Darpe, A.K.: A novel way to detect transverse surface crack in a rotating shaft. J. Sound Vib. **305**, 151–171 (2007)
18. Patel, T.H., Darpe, A.K.: Influence of crack breathing model on nonlinear dynamics of a cracked rotor. J. Sound Vib. **311**, 953–972 (2008)
19. Bachschmid, N., Pennacchi, P., Tanzi, E.: Some remarks on breathing mechanism, on non-linear effects and on slant and helicoidal cracks. Mech. Syst. Signal Process. **22**, 879–904 (2008)
20. Muñoz-Abella, B., Rubio, L., Rubio, P.: Stress Intensity factor estimation for unbalanced rotating cracked shafts by artificial neural networks. Fatigue Fract. Eng. Mater. Struct. **38**, 352–367 (2014)
21. Rubio, P., Rubio, L., Muñoz-Abella, B., Montero, L.: Determination of the stress intensity factor of an elliptical breathing crack in a rotating shaft. Int. J. Fatigue **77**, 216–231 (2015)
22. Blackburn, W.S.: Calculation of stress intensity factors for straight cracks in grooved and ungrooved shafts. Eng. Fract. Mech. **8**, 731–736 (1976)
23. Astiz, M.A.: An incompatible singular elastic element for two- and three-dimensional crack problems. Int. J. Fract. **31**, 105–124 (1986)
24. Carpinteri, A.: Stress intensity factors for straight- fronted edge cracks in round bars. Eng. Fract. Mech. **42**, 1035–1040 (1992)
25. Shih, Y.S., Chen, J.J.: Analysis of fatigue crack growth on a cracked shaft. Int. J. Fract. **19**, 477–485 (1997)
26. Couroneau, N., Royer, J.: Simplified model for the fatigue growth analysis of surface cracks in round bars under mode I. Int. J. Fatigue **20**, 711–718 (1998)
27. Levan, A., Royer, J.: Part-circular surface cracks in round bars under tension, bending and twisting. Int. J. Fract. **61**, 71–99 (1993)
28. Shih, Y.S., Chen, J.J.: The stress intensity factor study of an elliptical cracked shaft. Nucl. Eng. Des. **214**, 137–145 (2002)
29. Shin, C.S., Cai, C.Q.: Experimental and finite element analyses on stress intensity factors of an elliptical surface crack in a circular shaft under tension and bending. Int. J. Fract. **129**, 239–264 (2004)
30. Toribio, J., Alvárez, N., González, B., Matos, J.C.: A critical review of stress intensity factor solutions for surface cracks in round bars subjected to tension loading. Eng. Fail. Anal. **16**, 794–809 (2009)
31. Predan, J., Mocilnik, V., Gubeljak, N.: Stress intensity factors for circumferential semi-elliptical surface cracks in a hollow cylinder subjected to pure torsion. Eng. Fract. Mech. **105**, 152–168 (2013)
32. Lorentzen, T., Kjaer, N.E., Henriksen, T.K.: The application of fracture mechanics to surface cracks in shafts. Eng. Fract. Mech. **23**, 1005–1014 (1986)
33. Mackay, T.L., Alperin, B.J.: Stress intensity factors for fatigue cracking in high-strength bolts. Eng. Fract. Mech. **21**, 391–397 (1988)
34. Fonte, M.A., Freitas, M.M.: Semi-elliptical fatigue crack growth under rotating or reversed bending combined with steady torsion. Fatigue Fract. Eng. Mater. Struct. **20**, 895–906 (1997)
35. Chen, C., Dai, L.: Bifurcation and chaotic response of a cracked rotor system with viscoelastic supports. Nonlinear Dyn. **50**, 483–509 (2007)

36. Han, Q., Chu, F.: Parametric instability of a Jeffcott rotor with rotationally asymmetric inertia and transverse crack. Nonlinear Dyn. **73**, 827–842 (2013)
37. Zhang, B., Li, Y.: Six degrees of freedom coupled dynamic response of rotor with a transverse breathing crack. Nonlinear Dyn. **78**, 1843–1861 (2014)
38. Carpinteri, A.: Surface flaws in cylindrical shafts under rotary bending. Fatigue Fract. Eng. Mater. **21**, 1027–1035 (1998)
39. Dao, N.H., Sellami, H.: Stress intensity factors and fatigue growth of a surface crack in a drill pipe during rotary drilling operation. Eng. Fract. Mech. **96**, 626–640 (2012)
40. Rubio, L., Muñoz-Abella, B., Rubio, P., Montero, L.: Quasi-static numerical study of the breathing mechanism of an elliptical crack in an unbalanced rotating shaft. Lat. Am. J. Solids Struct. **13**, 2333–2350 (2014)
41. Carpinteri, A.: Shape change of surface cracks in round bars under cyclic axial loading. Int. J. Fatigue **15**, 21–26 (1993)
42. Lin, X.B., Smith, R.A.: Shape growth simulation of surface cracks in tension fatigued round bars. Int. J. Fatigue **19**, 461–469 (1997)
43. Toribio, J., Matos, J.C., González, B., Escuadra, J.: Numerical modelling of cracking path in round bars subjected to cyclic tension and bending. Int. J. Fatigue **58**, 20–27 (2014)
44. Forman, R.G., Kearney, V.E., Engle, R.M.: Numerical analysis of crack propagation in cyclic-loaded structures. J. Basic Eng. **89**, 459–464 (1967)
45. Madis, M., Beretta, S., Zerbst, U.: An investigation on the influence of rotary bending and press fitting on stress intensity factors and fatigue crack growth in railway axles. Eng. Fract. Mech. **75**, 1906–1920 (2008)
46. Hibbitt, Karlsson, Sorensen.: ABAQUS Theory manual, Version 6.7, Dassault systems Inc 3 712 (2007)
47. Rubio, L., Fernández-Sáez, J.: A new efficient procedure to solve the nonlinear dynamics of a cracked rotor. Nonlinear Dyn. **70**, 1731–1745 (2012)
48. Lin, X.B., Smith, R.A.: Fatigue growth simulation for cracks in notched and unnotched round bars. Int. J. Mech. Sci. **40**, 405–419 (1998)
49. Toribio, J., Matos, J.C., González, B., Escuadra, J.: Numerical modelling of crack shape evolution for surface flaws in round bars under tensile loading. Eng. Fail. Anal. **16**, 618–630 (2009)
50. Carpinteri, A., Ronchei, C., Vantadori, S.: Fatigue resistant design of round bars weakened by a V-shaped circumferential notch. Procedia Eng. **74**, 321–324 (2014)
51. Caspers, M., Mattheck, C., Munz, D.: Fatigue crack propagation in cylindrical bars. Z. Werkst. **17**, 327–333 (1986)
52. Carpinteri, A., Brighenti, R.: Part-through cracks in round bars under cyclic combined axial and bending loading. Int. J. Fatigue **18**, 33–39 (2009)
53. Fonte, M.A., Freitas, M.M.: Stress intensity factors for semi-elliptical surface cracks in round bars under bending and torsion. Int. J. Fatigue **21**, 457–463 (1999)
54. Cai, C.Q., Shin, C.S.: A normalized area-compliance method for monitoring surface crack development in a cylindrical rod. Int. J. Fatigue **27**, 801–809 (2005)
55. Khooand, S.W., Saravanan, K.: Stress intensity factor for cracks emanating from a shaft. J. Appl. Sci. **11**, 1839–1844 (2011)
56. Ismail, A.E., Ariffin, A.K., Abdullah, S., Ghazali, M.J.: Stress intensity factors for surface cracks in round bar under single and combined loadings. Meccanica **47**, 1141–1156 (2012)
57. Rubio, L., Montero, L., Munoz-Abella, B., Rubio, P.: Efecto de la presencia y orientación de una masa excéntrica en la forma del frente de una fisura de un eje rotatorio. Anales de Ingeniería Mecánica **19**, 1–8 (2012)
58. Carpinteri, A., Vantadori, S.: Sickle-shaped cracks in metallic round bars under cyclic eccentric axial loading. Int. J. Fatigue **31**, 759–765 (2009)
59. Carpinteri, A., Vantadori, S.: Sickle-shaped surface crack in a notched round bar under cyclic tension and bending. Fatigue Fract. Eng. Mater. Struct. **32**, 223–232 (2009)
60. Railway Investigation Report R10T0035, Transportation Safety Board of Canada (2010)